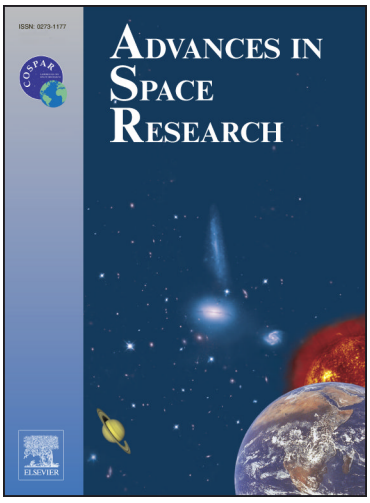

Equilibrium Positions on Stationary Orbits and Planetary Principal Inertia Axis Orientations for the Solar System

Pilar Romero, Gonzalo Barderas, Javier Mejuto

PII: S0273-1177(18)30130-3
DOI: https://doi.org/10.1016/j.asr.2018.02.015
Reference: JASR 13633

To appear in: *Advances in Space Research*

Received Date: 6 November 2017
Accepted Date: 13 February 2018

Please cite this article as: Romero, P., Barderas, G., Mejuto, J., Equilibrium Positions on Stationary Orbits and Planetary Principal Inertia Axis Orientations for the Solar System, *Advances in Space Research* (2018), doi: https://doi.org/10.1016/j.asr.2018.02.015

Equilibrium Positions on Stationary Orbits and Planetary Principal Inertia Axis Orientations for the Solar System

Pilar Romero[a,*], Gonzalo Barderas[b], Javier Mejuto[b]

[a] *Instituto de Matemática Interdisciplinar. Astronomía y Geodesia, Facultad de Matemáticas, Universidad Complutense de Madrid, E-28040 Madrid, Spain*
[b] *S.D. Astronomía y Geodesia, Facultad de Matemáticas, Universidad Complutense de Madrid, E-28040 Madrid, Spain*

Abstract

We present a qualitative analysis in a phase space to determine the longitudinal equilibrium positions on the planetary stationary orbits by applying an analytical model that considers linear gravitational perturbations. We discuss how these longitudes are related with the orientation of the planetary principal inertia axes with respect to their Prime Meridians, and then we use this determination to derive their positions with respect to the International Celestial Reference Frame. Finally, a numerical analysis of the non-linear effects of the gravitational fields on the equilibrium point locations is developed and their correlation with gravity field anomalies shown.

Keywords:
Principal inertia axes, Equilibrium point locations, Stationary orbits, Planetary gravitational fields, Prime Meridian

1. Introduction

The qualitative analysis of dynamical systems mainly focuses on asymptotic properties of solutions and trajectories, by firstly searching the equilibrium points, or fixed points. Many papers (see e.g. Blitzer et al. (1962);

*Corresponding author:
Email address: prp@mat.ucm.es (Pilar Romero)

Musen and Bailie (1962); Zhao and Liu (1991)) have contributed to the orbital resonance research in a non-spherical gravity field. It is well known that there exists four equilibrium points under the action of a truncated gravity potential that takes into account the effect of the second order harmonics. The linear stability of the equilibrium points is also well established, two of them are stable and the other two unstable (Morando, 1963).

Now, we present a comparative analysis between two methods to study the orbital resonance model in the 2D phase plane in a rotating second degree and order gravity field. First, variational principles are applied to discuss the main characteristics of the stationary motion, showing that the equilibrium positions are located at the planet principal inertia axes in the equatorial plane at the synchronous orbit. Secondly, from the equations that describe the gravitational perturbations on a longitudinal synchronous position a qualitative analysis is made to locate equilibrium positions. We then discuss how the principal inertia axis orientation corresponds with the localization of these equilibrium points. For the Earth, with the EGM2008 Earth potential degree 2 coefficients, it is also shown that the localization of these equilibrium points on the geostationary orbit coincides with the orientation of the Earth principal inertia axes derived by Chen and Shen (2010) and Chen et al. (2015) solving an eigenvalue/eigen-vector problem.

The equilibrium points of satellites on the Earth stationary orbit have been addressed in, for e.g., Morando (1963), Gedeon (1969), Kamel et al. (1973) and Lara and Elipe (2002). Afterwards, Mars stationary orbit stability has been discussed in Alvarellos (2010) and Silva and Romero (2013). The current Solar System exploration has provided gravitational models that offer the possibility to numerically determine the localizations of the equilibrium points for stationary orbits including the effects of higher order and degree harmonics, as Zhao et al. (2013) made for the geosynchronous orbital motion with a Hamiltonian formulation.

The paper is organized as follows: In section 2.1 we determine the equilibrium conditions as the stationary solutions of the equations of motion and the ideal stationary orbit for the Solar System planets. In section 2.2 we describe the linear gravitational perturbations due to the non-spherical part of the planet's gravity field. Using the available gravitational models, the location and classification of the equilibrium points is determined. In section 2.3, we use these qualitative analysis to place planetary principal inertia axes with respect to planetary prime meridians. The localization of the planetary principal inertia axes with respect the International Celestial Reference

Frame (ICRF) (Luzum et al., 2010) is given in section 2.4. The non-linear effects are examined in section 3 and the relationship between the equilibrium point locations and the planetary gravity field anomalies is analyzed. Finally, the main results are summarized in section 4.

2. Stationary motion

We discuss how to find the localization of the equilibrium points. First, using a body fixed reference frame with the coordinate axes aligned along the principal moments of inertia, and then, using a reference frame with the z-axis taken as the rotation axis and the x-axis coinciding with the Prime Meridian. The comparative analysis between both approaches allows to readily determine the orientation of the planetary principal inertia axes with respect to planetary conventional Prime Meridians.

2.1. Equilibrium conditions

The equilibrium conditions are determined as the stationary solutions of the equations of motion. These equations of motion can be derived as in Lara and Elipe (2002), using variational principles, in a rotating reference frame, $\{O; x, y, z\}$, with the coordinate axes parallel to the three main principal axes of inertia, and the origin, O, at the center of mass of the rotating planet, with constant angular velocity $\Omega_{\rm P}$ in the z-axis direction.

The Lagrangian of the motion, L, is expressed as the sum of kinetic energy, T, and the effective potential, W, defined as the combined gravitational potential, U, and the rotational potential terms, as follows:

$$\begin{aligned} L &= T + W = \frac{1}{2}(\dot{x}^2 + \dot{y}^2 + \dot{z}^2) + \Omega_{\rm P}(x\dot{y} - \dot{x}y) + \\ &+ U(x, y, z) + \frac{1}{2}\Omega_{\rm P}^2(x^2 + y^2). \end{aligned} \tag{1}$$

For a given mass point, with coordinates $(x,\ y,\ z)$, at a radial distance, $r = (x^2 + y^2 + z^2)^{1/2}$, the gravitational potential is:

$$U = \frac{\mu_{\rm P}}{r} + R, \tag{2}$$

where the second order and degree gravitational perturbing potential R is

$$\begin{aligned} R &= -\frac{\mu_{\rm P}}{r}\left(\frac{a_{\rm P}}{r}\right)^2 \left(J_{20}^* \frac{x^2 + y^2 - 2z^2}{2r^2} - \right. \\ &\left. - J_{22}^* \frac{3\,(x^2 - y^2)}{r^2}\right), \end{aligned} \tag{3}$$

where μ_{P} is the planet gravitational constant, a_{P} is the equatorial radius, and J_{20}^*, J_{22}^* should be the spherical harmonic coefficients computed with respect to the planet principal axes of inertia, being $K_{22}^* = 0$.

Under these assumptions,the equations of motion obtained from the Lagrangian L given in (1) are:

$$\begin{aligned} \ddot{x} - 2\,\Omega_{\mathrm{P}}\dot{y} + {\Omega_{\mathrm{P}}}^2 x + \frac{\partial U}{\partial x} &= 0, \\ \ddot{y} + 2\,\Omega_{\mathrm{P}}\dot{x} + {\Omega_{\mathrm{P}}}^2 y + \frac{\partial U}{\partial y} &= 0, \\ \ddot{z} + \frac{\partial U}{\partial z} &= 0. \end{aligned} \tag{4}$$

Since the necessary and sufficient conditions for the existence of equilibrium points are:

$$\ddot{x} = \ddot{y} = \ddot{z} = \dot{x} = \dot{y} = 0, \tag{5}$$

the equilibrium solutions are found by solving the following system of partial differential equations:

$$\begin{aligned} {\Omega_{\mathrm{P}}}^2 x + \frac{\partial U}{\partial x} &= 0, \\ {\Omega_{\mathrm{P}}}^2 y + \frac{\partial U}{\partial y} &= 0, \\ \frac{\partial U}{\partial z} &= 0, \end{aligned} \tag{6}$$

The solutions of (6) are the classical Lagrangian relative equilibria that satisfy (Lara and Elipe, 2002) that $z = 0$ and either $x = 0$ and $r\,(J_{20}^*, J_{22}^*) > a_s$ or $y = 0$ and $r\,(J_{20}^*, J_{22}^*) > a_s$, with $a_s = \mu_{\mathrm{P}}^{1/3}\Omega_{\mathrm{P}}^{2/3}$, which corresponds to the nominal stationary orbit for $R = 0$. Therefore, equilibrium positions are located at the planet principal inertia axes ($x = 0$ or $y = 0$) in the equatorial plane ($z = 0$) at the stationary orbit. The localization of the equilibrium points along the planetary principal inertia axes has also been discussed in Scheeres (2006) and Wang and Xu (2014 and 2016).

A stationary orbit can only be nominally achieved at an equatorial and circular orbit with a synchronous semi major axis, a_s, that equates the rotational period of the planet according to the Kepler third law in a spherical and homogeneous gravitational field. Table 1 gives the gravitational constants, μ_{P}, the rotational periods, P_{P}, the planet's angular velocity, Ω_{P}, that agrees

Table 1: Solar System planets parameters and stationary semi-major axis.

Planet	μ_P $(\times 10^{-5})$ $(km^3 s^{-2})$	P_P (h)	Ω_P $(\times 10^5)$ (s^{-1})	a_s (km)	a_P (km)	a_s/a_P
Mercury[a]	0.220318708	1407.6	0.1239	242896	2440	99.6
Venus[b]	3.248585921	-5832.5	0.0299	1536561	6051	253.9
Earth [c]	3.986004415	23.9345	7.2921	42164	6378.1363	6.6
Mars[d]	0.428283756	24.6229	7.0883	20428	3396	6.0
Jupiter[e]	1267.127	9.9250	17.5851	160020	71492	2.2
Saturn[f]	379.405	10.656	16.3788	112248	60268	1.9
Uranus[g]	57.945	-17.24	10.1237	82688	25559	3.2
Neptune[h]	68.36	16.11	10.8338	83513	24764	3.4

[a] From Smith et al. (2012).
[b] From Konopliv et al. (1999).
[c] From Pavlis et al. (2012).
[d] From Konopliv et al. (2011).
[e] From Folkner (2011), derived from reference therein Jacobson (2003).
[f] From Jacobson et al. (2006).
[g] From Jacobson et al. (2007).
[h] From Jacobson (2009).

with the orbital synchronous mean motion, n_s, and the corresponding stationary semi-major axis, a_s, as well as planetary radius, a_P, for the eight planets in the Solar System.

It can be noted that Mars rotates at about the same angular rate as the Earth does, but it has about 11% its mass, so the orbital radius of a stationary orbit at Mars will be smaller than that of the Earth with a value of 20428 km. The geostationary orbital radius is about 6.6 Earth radii, the Martian stationary orbital radius is very similar, at about 6 Mars radii. For other planets, for example for Venus, which is considerably less massive than Earth, due to its slowest rotation period, the stationary semi major axis is 1536561 km, about 254 times the planet radius. We note that this orbit is located outside the Venus sphere of influence, which radius is about 106 times the planet radius. This is also the case for Mercury, with a sphere of influence radius of 46 times the planet radius (Capderou, 2005).

2.2. Qualitative analysis of the perturbing gravitational effects on the equilibrium positions

We now consider a body-fixed reference frame with the origin at the mass center, the z-axis taken as the rotation axis and the x-axis coinciding with the Prime Meridian, so that the harmonic expansion of the planet's gravitational perturbing potential, R, in spherical coordinates $(r,\ \vartheta,\ \lambda)$, is

written as (Hofmann-Wellenhof and Moritz, 2006):

$$R = -(\mu_{\rm P}/r)\sum_{n=2}^{\infty}\sum_{m=0}^{n}(a_{\rm P}/r)^n \Big(J_{nm}R_{nm}(\vartheta,\lambda)+K_{nm}S_{nm}(\vartheta,\lambda)\Big), \quad (7)$$

where J_{nm} and K_{nm} are the spherical harmonic coefficients of degree n and order m, and $R_{nm}(\vartheta,\lambda)=P_{nm}(\cos\vartheta)\cos m\lambda$, $S_{nm}(\vartheta,\lambda)=P_{nm}(\cos\vartheta)\sin m\lambda$ the spherical harmonics with P_{nm} the associated Legendre polynomials.

A mass point in the stationary orbit is intended to be at rest with respect to a rotating planet. However, due to the gravitational perturbations R, it is shifted from its nominal position at longitude, l_s. The perturbations at the stationary orbit on the semi-major axis, a, and the mean longitude, l, can be obtained by means the linearized Lagrange equations given in Sidi (1997):

$$\frac{da}{dt} = \frac{2}{na}\frac{\partial R}{\partial l}, \quad (8)$$

$$\frac{dl}{dt} = n-\Omega_{\rm P}-\frac{2}{na}\frac{\partial R}{\partial a}, \quad (9)$$

where n is the perturbed orbital mean motion.

We can make a qualitative analysis of the equations system (8) and (9), as in Silva and Romero (2013), by introducing the auxiliary parameters α and β given by:

$$a = a_s(1+\alpha), \quad (10)$$

$$l = l_s+\beta, \quad (11)$$

thus, using the third law of Kepler and (10),

$$n=\mu^{\frac{1}{2}}a^{-3/2}=n_s-\frac{3}{2}n_s\alpha. \quad (12)$$

then, by substitution of the relations (10), (11) and (12) in equations (8) and (9), we obtain:

$$\frac{d\alpha}{dt} = \frac{1}{a_s}\frac{da}{dt}=\frac{1}{a_s}\frac{2}{na}\frac{\partial R}{\partial l}, \quad (13)$$

$$\frac{d\beta}{dt} = \frac{dl}{dt}=n_s-\Omega_{\rm P}-\frac{2}{na}\frac{\partial R}{\partial a}-\frac{3}{2}n_s\alpha. \quad (14)$$

Table 2: Second order and degree harmonic coefficients for the Solar System planets.

Parameter	Mercury[a]	Venus[b]	Earth[c]	Mars[d]	Jupiter[e]
$J_{20}\ (\times 10^3)$	0.05035422	0.00440444	1.08262617	1.95660888	14.696
$J_{22}\ (\times 10^6)$	−8.04790384	−0.55369451	−1.57461533	54.63038373	−0.005
$K_{22}\ (\times 10^6)$	−0.00542738	0.06166833	0.90387279	−31.59025869	0.010
K_{22}/J_{22}	0.00067438	−0.11137609	−0.57402768	−0.57825438	–
λ_{22}	−89.°980680	86.°822406	75.°071491	−14.°928509	–

[a] Derived from the normalized coefficients of the HGM007 gravity model (Mazarico et al. (2016), available at `pds-geosciences.wustl.edu/messenger/mess-h-rss_mla-5-sdp-v1/messrs_1001/data/shadr/ggmes_100v07_sha.tab` [*]).

[b] Derived from the normalized coefficients of the MGNP180U gravity model (Konopliv et al. (1999), available at `pds-geosciences.wustl.edu/mgn/mgn-v-rss-5-gravity-l2-v1/mg_5201/gravity/shgj180u.a01` [*]).

[c] Derived from the normalized coefficients of the EGM2008 gravity model (Pavlis et al. (2012), available at `http://icgem.gfz-potsdam.de/ICGEM/shms/egm2008.gfc` [*]).

[d] Derived from the normalized coefficients of the MRO120D gravity model (Konopliv et al. (2016), available at `http://pds-geosciences.wustl.edu/mro/mro-m-rss-5-sdp-v1/mrors_1xxx/data/shadr/jgmro_120d_sha.tab` [*]).

[e] Coefficients given in Folkner et al. (2017). The J_{22} and K_{22} coefficients are determined to be statistically zero as expected for a fluid planet in equilibrium.

[*] Accessed 06/Nov./2017.

Now, taking the perturbing potential (7) up to order and degree 2, with $r = a$, in the form given by Kamel et al. (1973):

$$R = -3J_{22}\frac{\mu_{\rm P}}{a}\left(\frac{a_{\rm P}}{a}\right)^2 \cos 2(l - \lambda_{22}), \tag{15}$$

with λ_{22} :

$$\lambda_{22} = \frac{1}{2}\tan^{-1}\left(\frac{K_{22}}{J_{22}}\right), \tag{16}$$

and considering the longitude drift, $\dot{l} = \frac{dl}{dt}$, equations (13) and (14) yield:

$$\ddot{l} = \frac{d\,\dot{l}}{dt} = -18J_{22}n_s^2\left(\frac{a_{\rm P}}{a_s}\right)^2 \sin 2(l - \lambda_{22}). \tag{17}$$

Finally, by imposing $\ddot{l} = 0$ in (17), the equilibrium points are determined:

$$\sin 2(l - \lambda_{22}) = 0. \tag{18}$$

The relative extrema for the function

$$F(l) = \int_{l_0}^{l} 18J_{22}n_s^2\left(\frac{a_{\rm P}}{a_s}\right)^2 \sin 2(l - \lambda_{22})dl \tag{19}$$

give the criteria to classify the four stationary points (Perko, 2001).

To numerically evaluate the equilibrium point longitudes using (16) and (18) the un-normalized harmonic coefficients J_{22} and K_{22} are needed. The Solar System gravitational models provide normalized harmonic coefficients $\bar{C}_{nm}$ and $\bar{S}_{nm}$ with respect to the planetary Prime Meridians. For Mercury, the NASA GSFC Hermean gravity field model, HGM007, has been obtained up to degree and order 100 using all MESSENGER tracking data up to the end of the mission. The reference longitude for the spherical harmonic expansion is the Mercury Prime Meridian, at 20° E from the crater Hun Kal (Archinal et al., 2011).

The JPL Venus, MGNP180U, spherical harmonics gravity solution (Sjogren, 1997; Konopliv et al., 1999) has been determined using Magellan Doppler radiometric tracking data. The model consists on normalized harmonics up to degree and order 180 in selected equatorial regions and referenced to the crater Ariadne Prime Meridian (Archinal et al., 2011).

The current Earth Gravitational Model EGM2008 has been released by the National Geospatial-Intelligence Agency (Pavlis et al., 2012). This gravitational model is complete to spherical harmonic degree and order 2159, and contains additional coefficients extending to degree 2190 and order 2159, referenced to Greenwich.

The JPL 120th degree and order Mars gravity model, MRO120D, includes tracking data from Mars Reconnaissance Orbiter, Mars Odyssey, Mars Global Surveyor, Pathfinder and Viking 1 and MER Opportunity landers (Konopliv et al., 2016). The Prime Meridian of this model matches the Mars Prime Meridian, Airy-0 (Archinal et al., 2011), at the J2000 epoch to about 1.6 meters.

The latest Jupiter gravity field includes the zonal harmonics up to degree 8, referenced to the Jupiter System III coordinate system (Archinal et al., 2011), based on Doppler data from the Juno spacecraft orbits (Folkner et al., 2017). As expected for a fluid planet in equilibrium, J_{22} and K_{22} coefficients are determined to be statistically zero. A non-zero J_{22} would be related to a possible solid core. Analysis on Jupiter's differential rotation could enable narrowing the range of internal structures and provide information about core mass, heavy element concentration, and density distribution as the Juno mission progresses (Kaspi et al., 2017). For the other Outer Planets, zonal harmonics are also known in the gravitational potential expansion, up to degree 8 for Saturn (Jacobson et al., 2006), and up to degree 4 for Uranus (Jacobson, 2014) and Neptune (Jacobson, 2009).

Table 3: Localization of the equilibrium points for the Solar System planets from the qualitative analysis. Gravitational potential up to order and degree 2.

Planet	Stable	Unstable	Stable	Unstable
Mercury	90.°019320	180.°019320	270.°019320	0.°019320
Venus	86.°822406	176.°822406	266.°822406	356.°822406
Earth	75.°071491	165.°071491	255.°071491	345.°071491
Mars	344.°980582	74.°980582	164.°980582	254.°980582

Table 2 lists the adopted numerical data for the second order and degree un-normalized harmonic coefficients derived using the relationships (Hofmann-Wellenhof and Moritz, 2006):

$$\begin{Bmatrix} \bar{C}_{nm} \\ \bar{S}_{nm} \end{Bmatrix} = -\sqrt{\frac{(n+m)!}{2\,(2n+1)\,(n-m)!}} \begin{Bmatrix} J_{nm} \\ K_{nm} \end{Bmatrix}. \tag{20}$$

Table 3 gives the longitudes of the equilibrium points from their respective Prime Meridians, derived from (18) using λ_{22} given in (16). There are two stable points and two unstable points.

The localization of the equilibrium points may be applied to orientate the planetary principal inertia axes.

2.3. Orientation of the planetary principal inertia axes with respect to planetary Prime Meridians

The qualitative analysis, made in the embedded phase space described by l and $\dot{l}$, allows us to readily place planetary principal inertia axes with respect to planetary conventional prime meridians. The dynamical meaning of the longitudinal equilibrium points may be visualized considering the equatorial dynamical shape of the planet. A non-zero J_{22} value is due to the dynamical equatorial elipticity whereas K_{22} will be zero if the planet Prime Meridian is in the direction of a principal axis of inertia. Thus, from equations (16) and (17), when the planet Prime Meridian is in the direction of the Ox principal inertia axis, the longitude of the first equilibrium point would be zero.

For the Earth, the equilibrium points localization yields the longitudes of $\lambda_{\mathrm{A}} = -14.°928509$ and $\lambda_{\mathrm{B}} = 75.°071491$ to orientate the Earth equatorial principal axes. We remark that these value are exactly the same as those obtained in Chen and Shen (2010) solving an eigenvalue-eigenvector problem on the basis of the degree-2 potential coefficients of the EGM2008 gravity model. Also, using the JGM-3 values of $J_{22} = -1.57454 \times 10^{-6}$ and $K_{22} =$

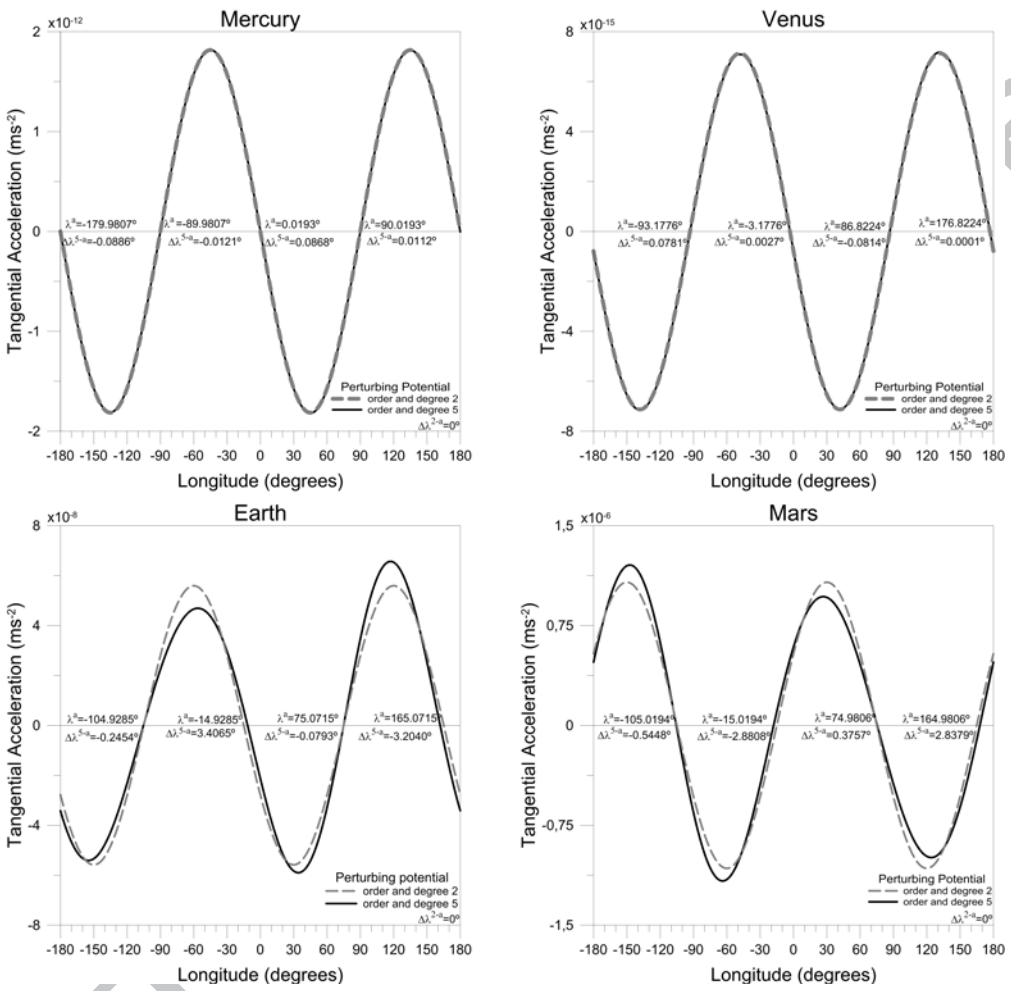

Figure 1: Comparison between planetary tangential accelerations for gravity field harmonic developments of order 2 and 5 at the stationary orbit. λ^{a} are the equilibrium point longitudes from the qualitative analysis, $\Delta\lambda^{2-\mathrm{a}}$ and $\Delta\lambda^{5-\mathrm{a}}$ their differences with order 2 and 5, respectively.

Table 4: Orientation of the planetary principal axes from Planetary Prime Meridians.

Parameters		Mercury	Venus	Earth	Mars
Orientations of	$\lambda_{\rm A}$	0.°019320	-3.°177594	-14.°928509	-105.°019418
Principal Axes	$\lambda_{\rm B}$	90.°019320	86.°822406	75.°071491	-15.°019418
Inertia Moments	A	0.069379	5.99330	8.0100255	0.26921
for whole planet	B	0.069386	5.99334	8.0101786	0.26921
($\times 10^{-37}$kg m^2)	C	0.069392	5.99340	8.0364114	0.27066
Normalized Polar Inertia Moment	$\frac{C}{Ma_{\rm P}^2}$	0.353	0.336	0.331	0.366

0.90387×10^{-6}, this procedure reproduces the longitude of the major axis of the equatorial ellipse of $\lambda_{\rm A} = -14.^{\circ}9291$ given in Groten (2000).

The estimated Earth's inertia moment values A, B, C are also in good agreement with those given in Chen et al. (2015). We use the dynamical ellipticity, H (Moritz and Mueller, 1987):

$$H = \frac{C - (A+B)/2}{C}, \tag{21}$$

with $H^{\rm Earth} = 3.2737634 \times 10^{-3}$ (Williams, 1994), and the relations (Hofmann-Wellenhof and Moritz, 2006):

$$J_{20} = \frac{C - (A+B)/2}{M_{\rm P}\ a_{\rm P}^2}, \tag{22}$$

$$J_{22} = \frac{A - B}{4 M_{\rm P}\ a_{\rm P}^2}, \tag{23}$$

with the Earth equatorial radius, $a_{\rm P}$, and Earth mass, $M_{\rm P}$, from Table 1, using a value of $G = 6.67259 \times 10^{-11}$ m^3 s^{-2} kg^{-1} (Groten, 2000); and J_{20} and J_{22} from Table 2. The obtained values are $A = 8.0100255$, $B = 8.0101786$ and $C = 8.0364114$ ($\times 10^{37}$ kg m^2).

Following this procedure, from the equilibrium points localization using equations (16) and (17), we have determined the right-handed orientations of the principal inertia axes for the inner solar system planets. Table 4 gives these orientations, as well as the values of their inertia moments. To this end we use the values of the normalized polar moment of inertia of $C^{\rm Mer}/(M_{\rm Mer}\ a_{\rm Mer}^2) = 0.353$ (Smith et al., 2012) for Mercury, and the values of the dynamical ellipticity of $H^{\rm Ven} = \frac{C-(A+B)/2}{C} = 1.31 \times 10^{-5}$ (Cottereau and Souchay, 2009) and $H^{\rm Mar} = \frac{C-(A+B)/2}{(A+B)/2} = 5.38 \times 10^{-3}$ (Hoolst and Dehant, 2002) for Venus and Mars, respectively. For comparison with a uniform

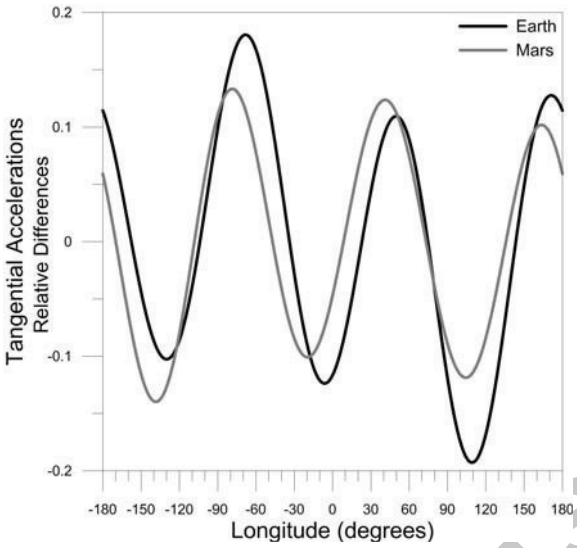

Figure 2: Tangential accelerations differences between order 2 and 5 scaled to their largest value for Earth and Mars.

sphere (C/Ma^2=0.4), Table 4 also lists the planetary normalized polar moment of inertia. Values $C/Ma_{\rm P}^2 < 0.4$ give an idea of the degree of concentration of masses towards their centers. The required values for the equatorial radius, masses, J_{20}, J_{22} and K_{22} are given in Tables 1 and 2.

2.4. Orientation of the planetary principal inertia axes with respect to the ICRF

The localization of the equilibrium points in Table 3 is given with respect to the Planetary Prime Meridians. Prime Meridian selection is always essentially arbitrary. Many different local places on Earth have been used until the nineteenth-century debate over a Prime Meridian adoption in order to get uniform standards of coordinates for cartographic purposes. Westernmost locations were selected in the early maps production, for instance Fuerteventura and Ferro in the Canary Islands, or Cape Verde and Azores Islands. Alternatively, justified by the existence of observatories, other places as Greenwich, Paris, the US Naval Observatory, Pulkovo or Stockholm, were concurrently used as Prime Meridian. Finally, after the International Meridian Conference held in 1884, the Airy transit circle of the Royal Greenwich Observatory, became the international standard for the Prime Meridian (see e.g. Howse (1980)). Prime Meridians for the inner Solar System planets are

defined in a conventional way (Archinal et al., 2011). On Mercury, the 20° W meridian is defined by the small impact crater Hun Kal –the Mayan number 20–, that references the planet's system of longitude. Mercury's early Prime Meridian was defined with a dynamical significance, based on the alignment of the principal inertia axis with the Sun direction at the first perihelion after 1 January 1950 (Margot, 2009). Hun Kal was selected because the 0° longitude region was shadowed when the Mariner 10 photographed it, concealing any near clear landmarks.

Using the early radar observations from Venus, Eve, the central peak of a crater located in Alpha Regio, was originally used to define zero longitude, so that the Central Meridian Longitude (CML) of Venus as observed from center of the Earth was 320.0° at 0 h on 20 June 1964 (Davies et al., 1980). After the Soviet Venera missions high-resolution radar mapping studies of Venus, in 1983, the Prime Meridian was redefined to pass through the central peak in the crater Ariadne.

Merton Davies' election of Airy-0 as the Prime Meridian on Mars was also arbitrary (Archinal and Caplinger, 2002; Duxbury et al., 2014). The German astronomers Wilhelm Beer and Johann Heinrich Mädler had chosen a small, bright circular feature as a reference point when they drew up the first map of Mars between the years 1830-32. Subsequently, in 1877, their choice was adopted as the zero meridian by the astronomer Giovanni Schiaparelli. Finally Airy-0, located in Sinus Meridiani along the line of Beer and Mädler, was chosen by Merton Davies as the Prime Meridian.

In the case of Jupiter, covered by highly reflective clouds, it was not so obvious how to choose a permanent feature. Initially, the solution was to define two coordinate systems, fixing the CML of the sub-Earth at the epoch 1897 Jul. 14 and two different rotation rates of 877.900 $^\circ/day$ (System I) and 870.270$^\circ/day$ (System II), corresponding to the cloud rotation for equatorial and higher regions (Dessler, 1983), respectively. In 1976, based on the rotation period of Jupiter's inner magnetosphere, a new longitude system (System III (1965)) was adopted. A rotation rate of 870.536 $^\circ/day$ and a CML of 217.595° from the Earth at the epoch 1965 Jan. 1 were selected (Seidelman and Divine, 1977). Prime Meridian definitions for Saturn, Uranus and Neptune are analogously based on the rotation of their magnetic fields (System III), although their rotational periods are not well known.

Table 5 lists the recommended values of the IAU Working Group on Cartographic Coordinates and Rotational Elements for the planetary Prime Meridian directions as the angle measured along the planets equator from

Table 5: Direction of the planetary Prime Meridians.

Parameter	Mercury	Venus	Earth	Mars
W_0 (deg)	329.5469	160.20	190.147	176.630
$\dot{W}$ (deg/day)	6.1385025	−1.4813688	360.9856235	350.89198226

the ascending node of the planets equator on the ICRF equator, W_0, and their main rates of change, $\dot{W}$ (Archinal et al., 2011). We note that for Mercury, on the basis of a new spin rate of $6\overset{\circ}{.}1385108$ Margot et al. (2012), a different value of $W_0 = 329\overset{\circ}{.}5988$ has been used in the HGM007 Hermean Gravity Model determination (Mazarico et al., 2016). Values listed in Table 6 give the relative positions of the planetary principal axis of inertia from planetary Prime Meridians, chosen as the reference meridian for its gravity field harmonic expansion. Shifting W_0 angles by the $\delta\lambda_{\mathrm{A}}$ values, we obtain the location of the planetary principal inertia axis with respect the ICRF.

Recent advances in modeling rotational theories extend rotational symmetric models to include the effects of triaxiality (see e.g. Chen and Shen (2010), Bizouard and Zotov (2013) and Gross (2015) for the Earth; Hoolst and Dehant (2002) for Mars; and by Cottereau and Souchay (2009) for Venus). The determined orientation of the principal inertia axis, could be useful for these studies on rotation.

3. Numerical analysis of high order harmonic effects in the equilibrium positions

To extend the analytical model presented in section 2, next we determine the equilibrium points by means of a numerical determination of the zero tangential acceleration localizations. Deriving the perturbing potential R given in (7), the tangential accelerations are calculated as

$$A_t = \frac{\partial R}{r\partial\lambda}, \tag{24}$$

using in R the un-normalized coefficients calculated with (20) from the gravitational potential models given in Mazarico et al. (2016) for Mercury, in Konopliv et al. (1999) for Venus, in Pavlis et al. (2012) for Earth and in Konopliv et al. (2016) for Mars.

We first consider the harmonic developments up to the same order and degree used in the analytical approach, i. e., $n = m = 2$. Thereafter, to improve the equilibrium points localization, we consider a higher order

Table 6: Relative positions of planetary principal axes of inertia from Prime Meridians.

Meridian Shift	Mercury	Venus	Earth	Mars
$\delta\lambda_A$	$0\overset{\circ}{.}0193$	$-3\overset{\circ}{.}1776$	$-14\overset{\circ}{.}9285$	$-105\overset{\circ}{.}0194$

and degree development up to $n = m = 5$. For these developments, Table 7 shows the localization of the equilibrium positions determined by numerically imposing $A_t = 0$ in (24) and taking $r = a_s$, where the numerical values of a_s are listed in Table 1.

For harmonics up to second order it can be seen that, as in the analytical approach, the locations are the same and the distribution of the stable/unstable equilibrium points is also symmetric. The equilibrium points location overlaps main planetary gravity field anomalies. Over two gravity lows, there are the two stable points; and over two gravity highs, the two unstable.

On Mercury, the 179.98° W unstable point is within two northern hemisphere significant anomalies, associated with some of the largest impact basins in the Solar System, such as the Caloris and Sobkou basins. The other unstable point is located near a hilly and lineated terrain at the antipode of the Caloris Basin, known as the Weird Terrain (Murray et al., 1974). Stable points are placed over the weaker negative anomalies, correlated with the topography depressions at ±90° from the Mercury Prime Meridian (Smith et al., 2012).

The equilibrium points localization on Venus is associated with the highest pronounced geoid elevation. The 180° W unstable point is at the intersection of multiple rift systems associated with dynamic activity at Atla Regio region, where the broad shield volcano Maat Mons is located (Jurdy and Stefanick, 1999).

Mars and Earth have completely different gravitational fields. Mars has a massive volcano zone, the Tharsis bulge, that contains the highest elevations on the planet and the largest known volcanoes in the Solar System, the Olympus Mons. This large accumulation of dense volcanic material deposited on one side is balanced on the other side by a wide gravity rise, the volcanic highland plane Syrtis Major Planitia, that give its gravitational field larger deviations from smoothness than Earth has. For $n = m = 2$, the longitudes are almost the same (Alvarellos, 2010; Silva and Romero, 2013). However, their similar λ_{22} values have opposite stable/unstable classification due to the different sign of the J_{22} coefficient of their respective gravitational potentials

Table 7: Solar System planets equilibrium points from the numerical method for gravitational potentials up to order n and degree m.

Planet	Stable		Unstable		Stable		Unstable	
	$n, m = 2$	$n, m = 5$	$n, m = 2$	$n, m = 5$	$n, m = 2$	$n, m = 5$	$n, m = 2$	$n, m = 5$
Mercury	$90.^{\circ}019320$	$90.^{\circ}030563$	$0.^{\circ}019320$	$0.^{\circ}106099$	$-89.^{\circ}980680$	$-89.^{\circ}992791$	$-179.^{\circ}980680$	$-180.^{\circ}069237$
Venus	$86.^{\circ}822406$	$86.^{\circ}740986$	$176.^{\circ}822406$	$176.^{\circ}822513$	$-93.^{\circ}177594$	$-93.^{\circ}099429$	$-3.^{\circ}177594$	$-3.^{\circ}174873$
Earth	$75.^{\circ}071491$	$74.^{\circ}992163$	$165.^{\circ}071491$	$161.^{\circ}867555$	$-104.^{\circ}928509$	$-105.^{\circ}173936$	$-14.^{\circ}928509$	$-11.^{\circ}522024$
Mars	$164.^{\circ}980582$	$167.^{\circ}818449$	$74.^{\circ}980582$	$75.^{\circ}356319$	$-15.^{\circ}019418$	$-17.^{\circ}900217$	$-105.^{\circ}019418$	$-105.^{\circ}564217$

(see Table 2).

When higher order harmonics effects are considered, the results for the Earth given in the Table 7 are in agreement with the equilibrium positions obtained in Zhao et al. (2013) using a Hamiltonian formulation to extend the orbital resonance model to include the combined effects of the harmonics J_{22}, J_{31} and J_{33} of the JGM3 Earth gravity model. For harmonics up to the fifth order, the results illustrate how the gravitational fields anomalies diminish the symmetry. These effects are neater on Earth and Mars due to their nearest stationary orbits with higher tangential accelerations. Figure 1 shows the estimation of the tangential accelerations for the different harmonics considered, of about 10^{-12}, 10^{-15}, 10^{-8}, and 10^{-6} $(m\,s^{-2})$ for Mercury, Venus, Earth and Mars, respectively.

Although Mars gravitational effects on its stationary orbit are 100 times greater than the corresponding Earth effects, it is interesting to note that the non-linear effects on the equilibrium points localization are greater for the Earth. Due to the geoid irregularities, Earth unstable points are shifted $3.^{\circ}4065$ and $-3.^{\circ}2040$ from their analytical localizations, whereas Mars stable points shifts are of $2.^{\circ}8379$ and $-2.^{\circ}8808$. The Figure 2 shows, for the Earth and Mars, the tangential accelerations differences between order and degree 2 and 5, scaled to their largest value of order 2. These relative differences explain the Earth greater non-linear effects on the symmetry loss in the equilibrium points location.

4. Conclusions

In this paper we have localized and classified the equilibrium points for the Solar System planets due to their gravitational field attractions. We have shown the relationship between the equilibrium positions with the orientation of the planetary principal inertia axes. Besides, we have determined the shifting values needed to match the planetary Prime Meridians with their principal inertia axis and their localizations with respect to the Inter-

national Celestial Reference Frame. Finally, non-linear effects on the equilibrium point localization have been evaluated. The differences are explained in terms of the tangential accelerations derived for gravity field harmonic developments of order 2 and 5 at the stationary orbit. The correlation of the planetary gravity field with the equilibrium point location has been analyzed. The results show the geographic locations of the stable points are tied to the greatest gravity anomalies, and the unstable points to the lowest gravity anomalies.

Acknowledgements

Part of this research has been funded by the Government of Spain (Project ESP2016-79135-R) and by Government of Comunidad de Madrid (Project CASI-CAM-CM S2013/ICE-2845).

References

Alvarellos, J. L., 2010. Perturbations on a stationary satellite by the longitude-dependent terms in Mars' gravitational field. Journal of the Astronautical Sciences 57, 701–715.

Archinal, B., AHearn, M., Bowell, E., Conrad, A., Consolmagno, G., Courtin, R., Fukushima, T., Hestroffer, D., Hilton, J., Krasinsky, G., Neumann, G., Oberst, J., Seidelmann, P., Stooke, P., Tholen, D., Thomas, P., Williams, I., 2011. Report of the IAU Working Group on Cartographic Coordinates and Rotational Elements: 2009. Celestial Mechanics and Dynamical Astronomy 109, 101–135.

Archinal, B. A., Caplinger, M., 2002. Mars, the Meridian, and Mert: The quest for Martian longitude. American Geophysical Union Fall Meeting, P22D–06.

Bizouard, C., Zotov, L., 2013. Asymmetric effects on Earth's polar motion. Celestial Mechanics and Dynamical Astronomy 116 (2), 195–212.

Blitzer, L., Boughton, E. M.and Kang, G., Page, R. M., 1962. Effect of the ellipticity of the equator on 24-hour nearly circular satellite orbits. Journal of Geophysical Research 67, 329–335.

Capderou, M., 2005. Satellites of Other Celestial Bodies. Springer Paris, Paris, pp. 453–494.

Chen, W., Li, J., Ray, J., Shen, W., Huang, C., 2015. Consistent estimates of the dynamic figure parameters of the Earth. Journal of Geodesy 89 (2), 179–188.

Chen, W., Shen, W., 2010. New estimates of the inertia tensor and rotation of the triaxial nonrigid Earth. Journal of Geophysical Research: Solid Earth 115 (B12), B12419.

Cottereau, L., Souchay, J., 2009. Rotation of rigid Venus: a complete precession-nutation model. Astronomy and Astrophysics 507 (3), 1635–1648.

Davies, M., Abalakin, V., Cross, C., Duncombe, R., Masursky, H., Morando, B., Owen, T., Seidelman, P., Sinclair, A., Wilkins, G., Tjuflin, Y., 1980. Report of the IAU Working Group on Cartographic Coordinates and Rotational Elements of the Planets and Satellites. Celestial Mechanics and Dynamical Astronomy 22, 205–230.

Dessler, A., 1983. Physics of the Jovian Magnetosphere. Cambridge University Press, Ch. Appendix B: Coordinate Systems, pp. 498–504.

Duxbury, T. C., Christensen, P., Smith, D. E., Neumann, G. A., Kirk, R. L., Caplinger, M. A., Albee, A. A., Seregina, N. V., Neukum, G., Archinal, B. A., 2014. The location of Airy-0, the Mars prime meridian reference, from stereo photogrammetric processing of THEMIS IR imaging and digital elevation data. Journal of Geophysical Research: Planets 119 (12), 2471–2486.

Folkner, W., 2011. Planetary ephemeris DE424 for Mars Science Laboratory early cruise navigation. JPL Interoffice Memorandum 343R-11-003, JPL.

Folkner, W. M., Iess, L., Anderson, J. D., Asmar, S. W., Buccino, D. R., Durante, D., Feldman, M., Gomez Casajus, L., Gregnanin, M., Milani, A., Parisi, M., Park, R. S., Serra, D., Tommei, G., Tortora, P., Zannoni, M., Bolton, S. J., Connerney, J. E. P., Levin, S. M., 2017. Jupiter gravity field estimated from the first two juno orbits. Geophysical Research Letters 44 (10), 4694–4700.

Gedeon, G. S., Jun. 1969. Tesseral Resonance Effects on Satellite Orbits. Celestial Mechanics 1, 167–189.

Gross, R., 2015. Theory of Earth rotation variations. International Association of Geodesy Symposia. Springer Berlin Heidelberg, pp. 1–6.

Groten, E., 2000. Parameters of common relevance of Astronomy, Geodesy, and Geodynamics. Journal of Geodesy 74 (1), 134–140.

Hofmann-Wellenhof, B., Moritz, H., 2006. Physical Geodesy. Springer-Verlag, Wien.

Hoolst, T. V., Dehant, V., 2002. Influence of triaxiality and second-order terms in flattenings on the rotation of terrestrial planets: I. Formalism and rotational normal modes. Physics of the Earth and Planetary Interiors 134 (1–2), 17 –33.

Howse, D., 1980. Greenwich Time And the Discovery of the Longitude. Oxford University Press, Oxford.

Jacobson, R., 2003. Jup230 orbit solution. NASA Planetary Data System.

Jacobson, R. A., 2009. The Orbits of the Neptunian Satellites and the Orientation of the Pole of Neptune. The Astronomical Journal 137 (5), 4322–4329.

Jacobson, R. A., 2014. The Orbits of the Uranian Satellites and Rings, the Gravity Field of the Uranian System, and the Orientation of the Pole of Uranus. stronomical Journal 148, 76–88.

Jacobson, R. A., Antreasian, P. G., Bordi, J. J., Criddle, K. E., Ionasescu, R., Jones, J. B., Mackenzie, R. A., Meek, M. C., Parcher, D., Pelletier, F. J., W. M. Owen, J., Roth, D. C., Roundhill, I. M., Stauch, J. R., 2006. The Gravity Field of the Saturnian System from Satellite Observations and Spacecraft Tracking Data. The Astronomical Journal 132 (6), 2520.

Jacobson, R. A., Campbell, J. K., Taylor, A. H., Synnott, S. P., 2007. The Gravity Field of the Uranian System and the Orbits of the Uranian Satellites and Rings. Bulletin of the American Astronomical Society 39, 453.

Jurdy, D. M., Stefanick, M., 1999. Correlation of Venus surface features and geoid. Icarus 139 (1), 93–99.

Kamel, A., Ekman, D., Tibbitts, R., 1973. East-West Stationkeeping Requirements of nearly Synchronous Satellites due to Earth's Triaxiality and Luni-Solar Effects. Celestial Mechanics 8, 129–148.

Kaspi, Y., Guillot, T., Galanti, E., Miguel, Y., Helled, R., Hubbard, W. B., Militzer, B., Wahl, S. M., Levin, S., Connerney, J. E. P., Bolton, S. J., 2017. The effect of differential rotation on jupiter's low-degree even gravity moments. Geophysical Research Letters 44 (12), 5960–5968.

Konopliv, A., Banerdt, W., Sjogren, W., 1999. Venus gravity: 180th degree and order model. Icarus 139 (1), 3–18.

Konopliv, A. S., Asmar, S. W., Folkner, W. M., Karatekin, A., Nunes, D. C., Smrekar, S. E., Yoder, C. F., Zuber, M. T., 2011. Mars high resolution gravity fields from MRO, Mars seasonal gravity, and other dynamical parameters. Icarus 211 (1), 401–428.

Konopliv, A. S., Park, R. S., Folkner, W. M., 2016. An improved JPL Mars gravity field and orientation from Mars orbiter and lander tracking data. Icarus 274, 253 – 260.

Lara, M., Elipe, A., 2002. Periodic orbits around geostationary positions. Celestial Mechanics and Dynamical Astronomy 82 (3), 285–299.

Luzum, B., Capitaine, N., Fienga, A., Folkner, W., Fukushima, T., Hilton, J., Hohenkerk, C., Krasinsky, G., Petit, G., Pitjeva, E., Soffel, M., Wallace, P., 2010. The IAU 2009 System of Astronomical Constants: the Report of the IAU Working Group on Numerical Standards for Fundamental Astronomy. Celestial Mech Dyn Astr 110, 293–304.

Margot, J.-L., 2009. A Mercury orientation model including non-zero obliquity and librations. Celestial Mechanics and Dynamical Astronomy 105, 329–33.

Margot, J.-L., Peale, S. J., Solomon, S. C., Hauck, S. A., Ghigo, F. D., Jurgens, R. F., Yseboodt, M., Giorgini, J. D., Padovan, S., Campbell, D. B., 2012. Mercury's moment of inertia from spin and gravity data. Journal of Geophysical Research: Planets 117 (E12), E00L09.

Mazarico, E., Genova, A., Goossens, S., Lemoine, F. G., Smith, D. E., Zuber, M. T., Neumann, G. A., Solomon, S. C., 2016. The gravity field of Mercury after MESSENGER. 47th Lunar and Planetary Science Conference, 2022.

Morando, B., 1963. Orbites de resonance des satellites de 24 heures. Bulletin Astronomique 24, 47–67.

Moritz, H., Mueller, I., 1987. Earth Rotation, Theory and Observation. Ungar Publishing Company, New York.

Murray, B. C., Belton, M. J. S., Danielson, G. E., Davies, M. E., Gault, D. E., Hapke, B., O'Leary, B., Strom, R. G., Suomi, V., Trask, N., 1974. Mercury's surface: Preliminary description and interpretation from mariner 10 pictures. Science 185 (4146), 169–179.

Musen, P., Bailie, A. E., 1962. On the motion of a 24-hour satellite. Journal of Geophysical Research 67, 11231132.

Pavlis, N. K., Holmes, S. A., Kenyon, S. C., Factor, J. K., 2012. The development and evaluation of the Earth Gravitational Model 2008 (EGM2008). Journal of Geophysical Research: Solid Earth 117, 1978–2012.

Perko, L., 2001. Differential Equations and Dynamical Systems. Springer-Verlag, New York.

Scheeres, D. J., 2006. Relative equilibria for general gravity fields in the sphere-restricted full 2-body problem. Celestial Mechanics and Dynamical Astronomy 94 (3), 317–349.

Seidelman, P., Divine, N., 1977. Evaluation of longitudes in System III (1965). Journal of Geophysical Research Letters 4 (2), 65–68.

Sidi, M. J., 1997. Space Dynamics and Control. Cambridge University Press, Cambridge, USA.

Silva, J., Romero, P., 2013. Optimal longitudes determination for the station keeping of areostationary satellites. Planetary and Space Science 87, 14–18.

Sjogren, W., 1997. MGNP180U spherical harmonic model. NASA Planetary Data System.

Smith, D. E., Zuber, M. T., Phillips, R. J., Solomon, S. C., Hauck, S. A., Lemoine, F. G., Mazarico, E., Neumann, G. A., Peale, S. J., Margot, J.-L., Johnson, C. L., Torrence, M. H., Perry, M. E., Rowlands, D. D., Goossens, S., Head, J. W., Taylor, A. H., 2012. Gravity Field and Internal Structure of Mercury from MESSENGER. Science 336 (6078), 214–217.

Wang, Y., Xu, S., 2014. Relative equilibria of full dynamics of a rigid body with gravitational orbit-attitude coupling in a uniformly rotating second degree and order gravity field. Astrophysics and Space Science 354 (2), 339–353.

Wang, Y., Xu, S., 2016. Orbital dynamics and equilibrium points around an asteroid with gravitational orbit-attitude coupling perturbation. Celestial Mechanics and Dynamical Astronomy 125, 265–285.

Williams, J. G., 1994. Contributions to the Earth's obliquity rate, precession, and nutation. Astronomical Journal 108, 711–724.

Zhao, C., Liu, L., 1991. Some discussions about the ideal resonance. Acta Astronomica Sinica 32, 268276.

Zhao, C.-Y., Zhang, M.-J., Wang, H.-B., Zhang, W., Xiong, J.-N., 2013. Two-dimensional phase plane structure and the stability of the orbital motion for space debris in the geosynchronous ring. Advances in Space Research 52 (4), 677 – 684.